Radiation Detection Technology and Methods (2023) 7:447–456
https://doi.org/10.1007/s41605-023-00397-x

ORIGINAL PAPER

Effect of annealing atmospheres on the scintillation properties of Ce^{3+}-doped YAG nanoscintillator

Billel Zahra[1,3] · Lakhdar Guerbous[2] · Hicham Bousbia-salah[3] · Allaoua Boukerika[2]

Received: 19 December 2022 / Revised: 27 February 2023 / Accepted: 8 March 2023 / Published online: 31 March 2023

Abstract

Background In this study, three sample detectors have been prepared by using cerium-activated YAG nanoscintillator ($Y_3Al_5O_{12}$: Ce^{3+}) synthesized by sol–gel method and heat-treat at 900 °C for 2 h in different atmospheres such as vacuum, air and nitrogen.

Purpose Many studies about YAG: Ce^{3+} single crystal have been carried out, but the material at the nanoscale remains not enough understood. The objective of the present paper is to investigate the effects of annealing atmosphere on the scintillation properties and identify the suitable atmosphere that allow to design radiation detectors with high scintillation efficiency.

Methods In order to accurately assess the scintillation properties, the nanoscintillator sample powders have been designed as a detector, in which, preparation operations such as surface homogenization and efficiency coupling with photomultiplier tube (PMT) window were developed. The study was performed using γ-rays 662 keV released from ^{137}Cs radioactive source, the bi-alkali GDB-4FF PMT was used as a photodetector. Nuclear instrumentation chain was set up in order to collect the pulse height spectra, NaI:Tl single-crystal scintillator was used as a reference detector to estimate the scintillation light yield. The delayed coincidence method was used for measuring the scintillation decay time of nanoscintillator sample detectors.

Results The sample detector annealed at vacuum atmosphere exhibits the best scintillation properties, the scintillation light yield was estimated to be $14{,}600 \pm 3400$ ph/MeV and the fast component in the scintillation decay was 90 ns.

Conclusion The vacuum is the suitable atmosphere which allows the development of radiation detectors with high scintillation efficiency.

Keywords Nanoscintillator YAG: Ce^{3+} · Scintillation properties · γ-rays 662 keV · Photomultiplier tube · Sample detectors · Annealing atmosphere

Introduction

Yttrium aluminum garnet (YAG, $Y_3Al_5O_{12}$) is extensively used as laser materials, it has been widely studied in the last decades. Due to its good mechanical, chemical and optical properties, YAG-based materials are used for many applications such as in cathode-ray tubes, field emission displays, scintillation, phosphorus, electro-luminescent applications and optical windows [1–4]. However, one of the most important applications of YAG: Ce^{3+} phosphor is radiation detection because of its high sensitivity, high density (4.56 g/cm^3), high temperature creep resistance and fast decay [5–9]. Many studies and researches have been achieved on the structural, morphological and luminescence properties of $Y_3Al_5O_{12}$: Ce^{3+} nanopowder to improve the crystal quality [10–16]. Jiuping et al. [17] studied the effect of annealing atmosphere on the luminescence and scintillation properties of $Lu_3A_{l5}O_{12}$: Ce^{3+} single crystal, significant effect of the annealing treatment on the luminescence and scintillation properties was observed. Furthermore, Chen et al. [18] investigated the effect of annealing atmosphere on scintillation properties of GYGAG: Ce, Mg scintillator ceramics; in their report, the ratio of Ce^{4+}/Ce^{3+} in the

✉ Billel Zahra
billel.zahra@g.enp.edu.dz

1 Electronic Department, Nuclear Research Center of Birine (CRNB), BP 180, Ain Oussera, Djelfa, Algeria

2 Physics Division, Nuclear Research Center of Algiers (CRNA), Algiers 02, Bd Frantz Fanon, BP 399, 16000 Algiers, Algeria

3 Electronic Department, National Polytechnic School (ENP), 10 Rue des Frères Oudek, BP 182, 16200 El-Harrach, Algiers, Algeria

GYGAG: Ce, Mg ceramic increased after the annealing in oxygen atmosphere and leading to the improvement of the scintillation efficiency. However, no report about the effect of annealing atmosphere on the scintillation properties of YAG: Ce^{3+}synthesized at the nanoscale.

Currently, single-crystal YAG is most widely used in radiation detection applications. Kim et al. [6] have investigated the scintillation properties of YAG: Ce^{3+} single crystal under ^{137}Cs gamma radiation source, in their report, the energy resolution was determined to be 14% full width half maximum (FWHM), the light yield was estimated to be 20,800 ± 4000 ph/MeV and the measured decay time was 112 ns. Furthermore, Chewpraditkul et al. [19] conducted a comparative study of LuAG: Ce and YAG: Ce single crystals under 662 keV γ-rays, for the YAG: Ce, the energy resolution was measured to be 7% and the photoelectron yield was 3750 ± 200 ph/MeV. The fast decay time and the coincidence timing resolution were 96 ns and 660 ps, respectively. Growing single-phase crystal is highly cost intensive, requiring highly pure chemicals, highly sophisticated laboratory and long processing time [20–23]. Chemical methods as sol–gel combustion [24], co-precipitation [25], solvothermal [26] and sol–gel method [27, 28] have been employed for the synthesis of YAG: Ce^{3+} powders. The sol–gel method provides an advantageous approach to fabricating low-cost scintillators with high purity, precise control over grain size and morphology, excellent luminescence properties and the ability to process at low temperatures [28]. In fact, actually, the concept of nanoscintillators started being developed due to their strong enhancement in light emissions, this improvement can be achieved by the optimization of some synthesis parameters [29–31]. Furthermore, the parameters of elaboration as the pH of the solution, the activator concentration, the annealing temperature and the annealing atmosphere are very important and they have a significant effect on the powder characteristics [28, 32, 33].

In addition, actually, the novel deep photo-dynamic therapy (PDT), which is very spectacular minimally invasive therapeutic method used in medical filed [34–37], constitutes another promising tool in cancer treatment. This method requires nanoscintillators with high light yield to be conjugates with a photosensitizer to produce therapeutically relevant results [38]. Indeed, several rare-earth ions-doped nanoparticle scintillators have been synthesized and studied as potential light sources for PDT system [39]. Garnet nanoscintillators are among them, such as Pr^{3+}-doped YAG [40] and Ce^{3+}-doped GAG [41].

In this work, YAG: 0.5% Ce^{3+} nanopowders synthesized by sol–gel method and heat-treat at 900 °C for 2 h at different atmospheres (vacuum, air and nitrogen) were used to design sample detectors, the objective is to study the effect of the annealing atmospheres on scintillation properties and identify the suitable atmosphere that allow to design a radiation detector with high performance.

For doing so, nuclear instrumentation chain was set up, the designed sample detectors were coupled with GDB-4FF PMT used as a photodetector, and the samples were excited by γ-662 keV from ^{137}Cs radioactive source. The relative light yield can be determined from the collected spectra. For the scintillation decay time measurement, the delayed coincidence technique was used [42, 43].

Experiment and methods

Pulse height spectra measurement

One of the most important analytical measurements for determining the performance of scintillating materials is pulse height spectra. Collecting these data allows us to determine the efficiency of the material in terms of the visible light produced via the scintillation mechanism. The experimental setup used for recording the pulse height spectra of the prepared samples is shown in the schematic diagram depicted in Fig. 1, the produced light under γ-ray excitation from ^{137}Cs source (662 keV) was readout by using bi-alkali GDB-4FF PMT, manufactured by the Beijing Comprehensive Instrument Factory and powered at 1500 V. For the

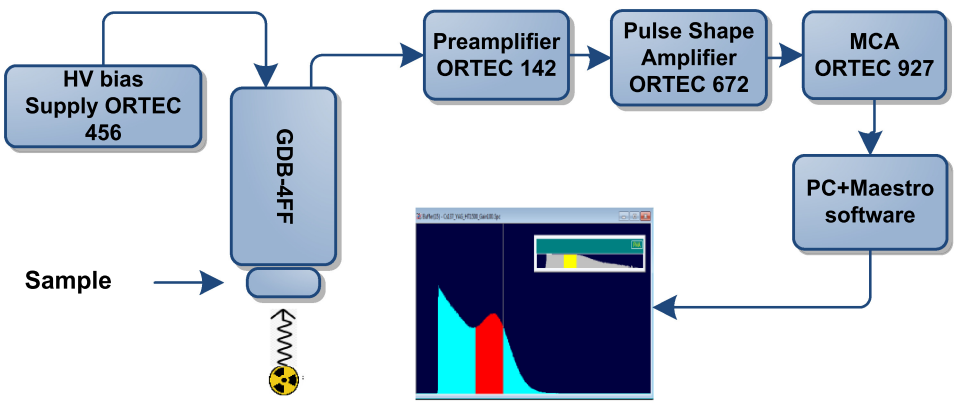

Fig. 1 Schematic view of the experimental setup for measuring the pulse height spectra of the prepared sample detectors

setup of nuclear electronic system high-voltage power supply ORTEC 465, preamplifier ORTEC 142PC, pulse shape amplifier ORTEC 672, multichannel analysis MCA ORTEC 927-ASPEC and PC with Maestro software were used, the PMT was placed in closed box for all measurements. Absolute light output and energy resolution measurements were made using the recorded height pulse spectra.

Details of sample detector design

Three sample detectors have been developed based on the YAG: 0.5% Ce^{3+} nanopowder synthesized by sol–gel method and heat-treat at 900 °C for 2 h at different annealing atmospheres, namely vacuum (10^{-6} mbar), air (atmospheric pressure) and nitrogen (N_2, 99.999%), the pH value of the solution has been stabilized at 1. The final shape was obtained by using two kinds of Mylar, the face to be coupled with the PMT window was covered by transparent Mylar which was used as a substrate, the opposite face was covered by the aluminized Mylar which was used as a reflector to prevent light loss, and the sides of the sample were wrapped by the aluminum foil. In order to fix the powder and get homogeneous distribution, we sprinkle pure ethanol on the substrate before laying the YAG powder. Figure 2 shows a photography of the designed samples.

For simplification, in all that follows, the prepared sample detectors Ce^{3+}-doped $Y_3Al_5O_{12}$ (YAG) were named as YAG_Nitrogen, YAG_Air and YAG_Vacuum according to the annealing atmosphere used during the synthesis process.

Optimal sample thickness selection

The thickness of the sample detectors developed from YAG: 0.5% Ce^{3+} nanopowder has a significant effect on its scintillation properties. It is typically chosen based on a compromise between several factors. These factors include the desired sensitivity of the detector, the energy range to be detected, the resolution of the detector, the scintillation light yield and attenuation length of the scintillator material.

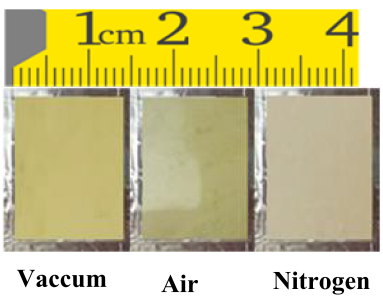

Fig. 2 Photography of the prepared sample detectors

YAG: Ce^{3+} nanopowder scintillators typically have high light yield and short attenuation lengths, which can result in high sensitivity and good energy resolution. However, if the thickness of the sample is too high, the light yield may be reduced due to self-absorption and scattering problem. Additionally, transparency is an important consideration when selecting the optimal thickness. In fact, YAG: Ce^{3+} nanopowder is an opaque material, which means that it does not allow light to pass through it easily. On the other hand, for very thin samples, the total energy absorption may be lower due to the reduced probability of interactions between the radiation and the sample material.

In order to determine the optimal thickness of the sample in terms of produced light yield, four sample detectors with different thicknesses, namely 0.5, 1, 2 and 3 mm, have been prepared using YAG: Ce^{3+} nanopowder annealed under vacuum. The energy spectra of γ-rays from a ^{137}Cs radioactive source were collected using the developed nuclear instrumentation system (Fig. 1) and the prepared sample detectors. The results of this experiment are presented in Fig. 3. It is important to indicate that the spectra were collected under identical and optimal experimental conditions, with a fixed high voltage of 1500 V, a shaping time of 3 µs and an amplification gain of 200.

The results show that the sample detectors with thicknesses of 2 and 3 mm exhibited transparency and self-absorption issues, resulting in a significant reduction in scintillation light output. In addition, the measured spectra did not show a photoabsorption peak for these thicker samples in contrast to the 0.5 and 1 mm samples. Furthermore, the scintillation efficiency of the sample with a thickness of 1 mm was slightly better than that of the sample with a thickness of 0.5 mm. Consequently, a thickness of 1 mm

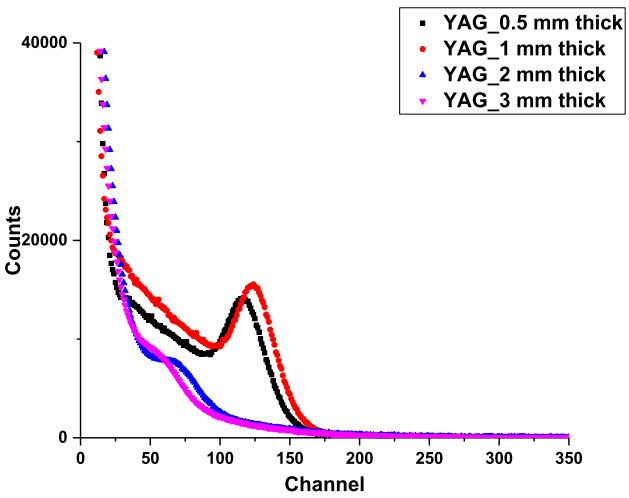

Fig. 3 Energy spectra of γ-rays from ^{137}Cs obtained using sample detectors prepared with different thicknesses of YAG: 0.5% Ce^{3+} powder annealed at vacuum

was selected for designing the Ce^{3+}-doped $Y_3A_{l5}O_{12}$ sample detectors. The final dimensions used for studying the effect of different annealing atmospheres on scintillation properties are $20 \times 15 \times 1$ mm^3.

Scintillation decay time measurement

The decay time measurements were done by using the method of a Thomas–Bollinger single-photon method [42], using fast-slow coincidence setup. For this setup, the two faces of each sample were covered by transparent Mylar. Therefore, the emitted light from the sample can be detected using two photomultiplier tubes PMTs. The schematic of the experiment is shown in Fig. 4. In this experiment, two PMTs were used, the first one was GBD-4FF used for the fast channel, the sample detector was coupled with this PMT, and the second was Dumont 6292 PMT used for the slow channel, it was placed opposite to GDB-4FF at a distance of 10 cm. The time difference between the signal generated in the GDB-4FF and the signal generated by the single photon detected in the second PMT (Dumont 6292) was measured using the CANBERRA Time-to-Amplitude converter model 2145 (TAC). The events were collected by ORTEC 927 MCA, the sample was irradiated by ^{137}Cs radioactive source.

Results and discussion

Scintillation light yield

The scintillation light yield (SLY) is one of the key scintillator parameters, it shows the efficiency of the scintillator to convert absorbed radiation energy to photons. It is defined as the number of photons N_{phe}, per unit of ionizing energy (ph/MeV), the measurement of the light yield of scintillator is not easy because of many considerations [44]. Different results have been found in the studies for the most popular crystals, e.g., NaI(Tl) and CsI(Tl), it depends on several causes such as the crystal growth method and the technique used to determine the light output.

In the present work, the method of comparison is used to measure the relative light yield (RLY%) of the sample detectors [45–47]. The NaI: Tl single-crystal scintillator is used as a reference detector, the formula is given in Eq. (1)

$$\mathrm{RLY}(\%) = \frac{\mathrm{PP_S}}{\mathrm{PP_R}} * \frac{G_\mathrm{R}}{G_\mathrm{S}} * \frac{Q_\mathrm{R}}{Q_\mathrm{S}} \tag{1}$$

where $\mathrm{PP_R}$ and $\mathrm{PP_S}$ are the peak positions of the reference detector and sample detector, respectively, G_R and G_S are,

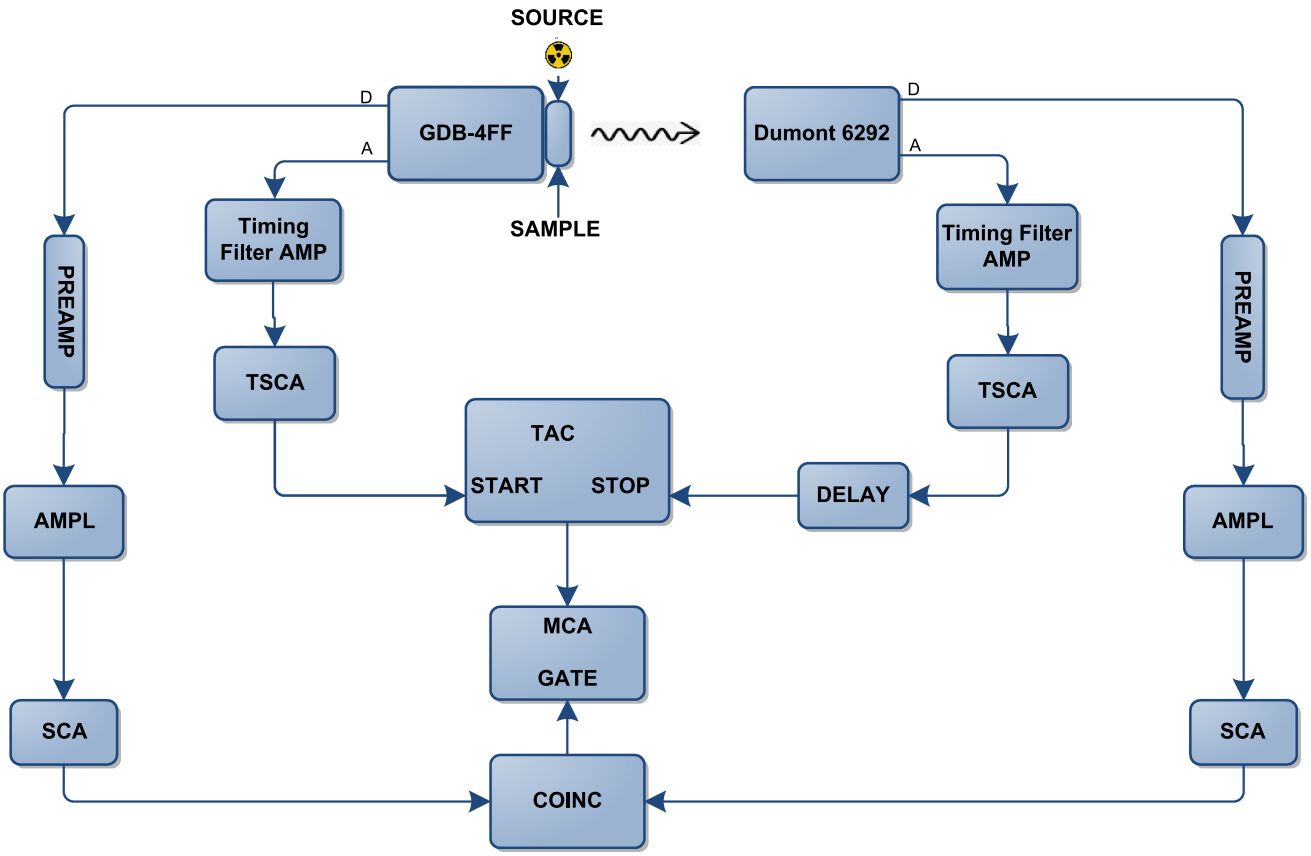

Fig. 4 Block diagram of the experimental setup used for the decay time measurement

respectively, the gains applied in the reference detector and the sample detector, $Q_R = 27.6$ % and $Q_S = 26.7$ %, are, respectively, the quantum efficiency of the GDB-4FF PMT over the spectral emission of the reference detector and studied sample detectors.

Firstly, in order to check the radiation response of the designed sample detectors for different gamma energy levels, the sample YAG_vacuum was used to collect the pulse height spectra of γ-rays from ^{137}Cs, ^{22}Na and ^{57}Co radioactive sources with 662, 511 and 122 keV gamma energy, respectively. The results are presented in Fig. 5a. Therefore, the energy-channel calibration curve was plotted, as shown in Fig. 5b. From the plot, one can observe that the energy versus channel values were well adjusted with a linear function. Secondly, in order to evaluate the effect of the annealing atmospheres on the SLY, the pulse height spectra of sample detectors and reference detector are collected under

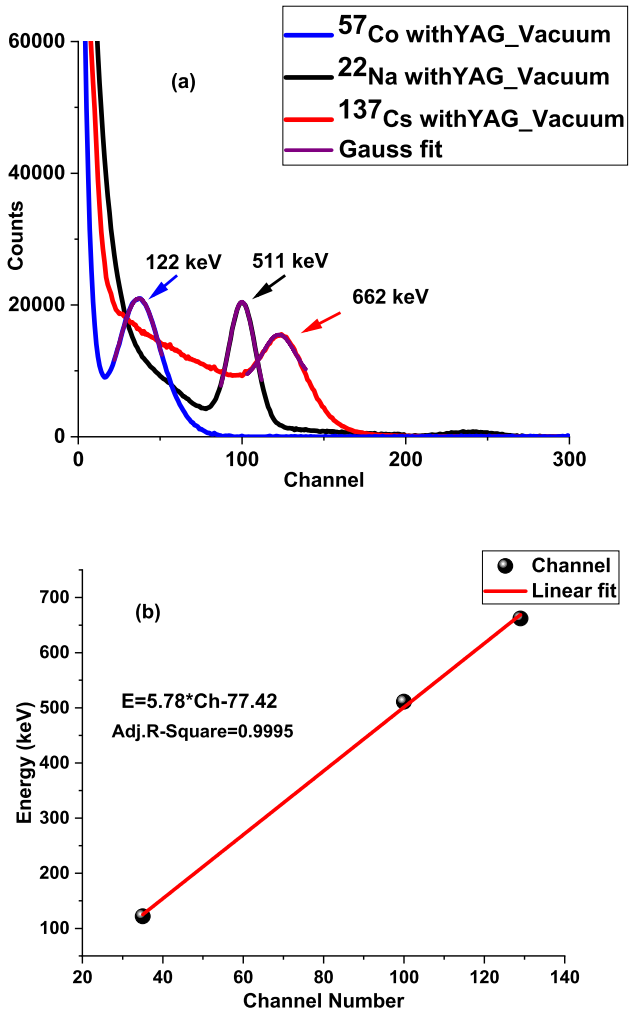

Fig. 5 **a** Pulse height spectra of γ-rays from ^{137}Cs, ^{22}Na and ^{57}Co radioactive sources using YAG_Vacuum sample detector and **b** Energy-channel calibration curve

662 keV γ-ray from ^{137}Cs radioactive source with 26.1 KBq and presented in Fig. 6, well-defined photo-peaks can be clearly observed, the shaping time was set at 3 µs, the high voltage was fixed at 1500 V for all the samples and even for the reference detector, G_R and G_S were fixed at 100 and 200, respectively.

The pulse height spectra (Fig. 6) were fitted with Gaussian function to determine the centroid and the FWHM of the photo-peaks, the results show that the sample annealed at vacuum exhibits the higher light yield.

The relative light output of the sample detectors can be determined by comparing the peak positions of the samples with that of NaI(Tl) single crystal using the collected pulse height spectra. The light yield of NaI:Tl was estimated to be 40,000 ± 8000 ph/MeV [48]. Consequently, the absolute light yield (ALY) of the sample detectors was calculated. Table 1 summarizes the obtained results.

According to the obtained results, it was noted that the annealing atmosphere has a significant effect on the scintillation light yield, the sample detector prepared from nanopowder YAG: Ce^{3+} annealed under vacuum atmosphere exhibits higher light output compared to the others (air and nitrogen). In our previous work [33], the average crystallite size of the

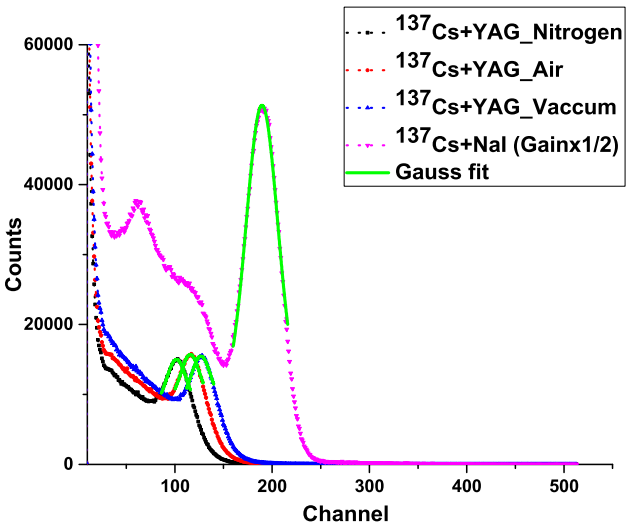

Fig. 6 Pulse height spectra of γ-rays from ^{137}Cs with Gaussian fit of sample detectors and reference detector

Table 1 Effect of annealing atmospheres on the scintillation light yield of YAG: 0.5%Ce

Annealed atmospheres	Peak positions	RLY (%)	ALY (ph/MeV)
YAG_Nitrogen	100.21	27	10,900 ± 2200
YAG_Air	117.23	32	12,800 ± 2800
YAG_Vacuum	129.15	35	14,600 ± 3400
NaI:Tl	189.18	100	40,000 ± 8000

three samples, calculated through the Scherrer formula, is approximately 18, 20 and 31 nm corresponding to nitrogen, air and vacuum, respectively. It was observed that the YAG: Ce^{3+} nanophosphor annealed in vacuum atmosphere had the largest value of the crystallite size. In fact, the crystallite size of nitrogen annealing is smaller than that of air and vacuum annealing, because the micro-strain contributions in the nitrogen are more pronounced, making a difference in crystallite growing speed, which is greater in vacuum than in air and nitrogen. Furthermore, a high photoluminescence (PL) emission intensity was observed for large crystallite size, which means a linear relation between crystallite size and PL emission intensity for this nanophosphor. In this study, we observe that the SLY increases with crystallite size of the samples as shown in Fig. 7 and Table 2. This result could be due to the influence of the defects density at grain boundaries. In fact, for the small crystallite size obtained with nitrogen annealing atmosphere, the surface-to-volume ratio (S/V) increases compared to the bigger size obtained with air and vacuum atmosphere, which lead to the increase of the defects density at grain boundaries. A higher defects density aids the non-radiative recombination of electron–hole pairs that may reduce the scintillation efficiency. Thus, the experimental results, obtained in this study, are relative under finite boundary conditions. In addition, the vacuum is clean atmosphere which can provide clean reaction conditions; therefore, the calcination in such atmosphere allows to get YAG: Ce^{3+} nanophosphors with less defects, which otherwise will act as non-radiative relaxation centers and perfect incorporation of Ce^{3+} ions into the Y lattice [33]. Moreover, the annealing atmospheres affect the concentration of oxygen vacancies and the reduction degree of Ce^{4+} to Ce^{3+} in YAG host [17, 18], which can be responsible to the increase of the SLY.

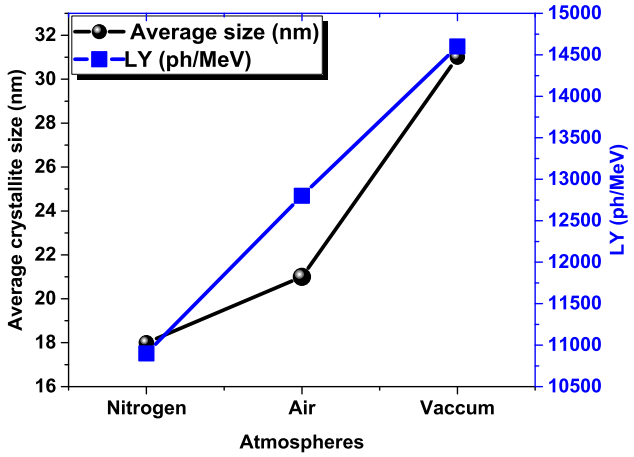

Fig. 7 Light yield and crystallite size relationship under different annealing atmospheres

Furthermore, it is known that the number of photons N_{phe} produced in the scintillation conversion process per energy E under X or γ-rays excitation can be expressed as [49]:

$$N_{phe} = \frac{E}{\beta E_g} \times S \cdot Q \tag{2}$$

where E_g is the band gap of the material, S and Q are, respectively, the quantum efficiencies of the transport and luminescence stages, and β is a phenomenological parameter which, for most materials, is typically between 2 and 3. If we consider E_{vis} as the photon energy in UV or visible generated, the relative efficiency can then be obtained as [50]:

$$\eta = \frac{E_{vis}}{E} \times N_{phe} \tag{3}$$

In fact, the experimentally determined scintillation light yield is generally inferior to the value given by Eq. (2) and it represents just a small fraction of generated photons, arriving to the PMT within a certain time gate or shaping time. In addition, interaction of X or γ-rays with nanoscintillator materials can lead to changes of the scintillation parameters. In fact, it was well established that reducing size can affect the value of the gap and therefore the luminescence yield Q in the non-doped semiconductor scintillator materials, but no quantum confinement effect was observed for doped inorganic scintillators nanomaterials [51]. However, the structural effects generating crystal-field fluctuations in nanoscale can influence the Q value. The energy transfer efficiency S can be affected through the presence of surface defects which become very critically at nanoscale. The understanding of different effects, which can influence the conversion of gamma energy to visible light photons and therefore improve the nanoscintillator *SLY*, is important challenge.

Table 2 Different calculated values of R, N_{phe}, R_M and R_i for different annealing atmospheres

Atmospheres	YAG_Nitrogen	YAG_Air	YAG_Vacuum
Crystallite size (nm)	18 ± 0.14	20 ± 0.75	31 ± 0.59
R (%)	25 ± 0.22	17 ± 0.15	13 ± 0.14
LY (Ph/MeV) (@662 keV)	10,900 ± 2200	12,800 ± 2800	14,600 ± 3400
N_{phe} (@662 keV)	1926	2262	2580
R_M (%)	5.76	5.32	4.98
R_i (%)	24.32	16.14	12.01

Table 3 Scintillation decay and rise time of YAG: Ce^{3+} sample detectors at different annealing atmospheres

Samples	Decay components				Rise time τ_r (*ps*)
	Fast		Slow		
	τ_f (*ns*)	Intensity (%)	τ_s (*ns*)	Intensity (%)	
YAG_Nitrogen	130 ± 7	18	640 ± 40	82	2307 ± 18
YAG_Air	104 ± 4	39	605 ± 20	61	2202 ± 27
YAG_Vacuum	90 ± 1.2	63	435 ± 14	37	2054 ± 25

Energy resolution

In radiation detection applications, energy resolution is one of the most important characteristics of the detector, it measures how precisely the energy of incoming particles can be determined. When a scintillator is subjected to different energy radiation, it must be able to distinguish the sources by having a different response according to the energy of the incident photon. Therefore, the energy resolution is the capability of the scintillator to distinguish two photons of near energies. Generally, four contributions to the energy resolution R are considered [52]:

$$R^2 = R_{np}^2 + R_{inh}^2 + R_p^2 + R_M^2 \tag{4}$$

where: R_p: transfer resolution, which can be ignored in case of PMT readout. R_M: photomultiplier resolution: is the statistical contribution due to the variance in the number of detected photons N_{phe} plus the variance due to the electron multiplication in the PMT, R_{inh}: is connected with inhomogeneity of the crystal quality causing local variations in the scintillation light output and R_{np}: is the contribution of the non-proportional response of the scintillator. A so-called nonlinear material will therefore have a light yield which will depend on the energy of the incident photon. The intrinsic resolution R_i results from the contribution of R_{inh} and R_{np}, it is defined as:

$$R_i^2 = R_{np}^2 + R_{inh}^2 \tag{5}$$

The processing of the data presented in Fig. 6 allows to calculate the energy resolution R of each sample detector under 662 keV γ-ray from ^{137}Cs radioactive source. The results are summarized in Table 2.

Furthermore, R_M can be estimated if the number of photoelectrons (N_{phe}) generated in the photodetector for a gamma-ray event in the scintillator is known. In fact, N_{phe} can be estimated as [53]:

$$N_{phe} = LY \times E_\gamma \times \eta_{det} \tag{6}$$

where LY is the light output of the scintillator (in photons/MeV), E_γ is the energy of the incident gamma-ray in MeV (0.662 in this case), η_{det} is the quantum efficiency of the photodetector over the emission spectrum of the scintillator taken as 26.7%. Furthermore, the statistical contribution R_M can be estimated using the traditional Poisson distribution [53, 54]:

$$R_M^2 = (2.36)^2 \times \frac{ENF}{N_{phe}} \tag{7}$$

where ENF is the excess noise factor of the photodetector (~ 1.15 for PMTs) [55]. Then, one can estimate N_{phe}, R_M and the intrinsic resolution R_i values of the studied sample detectors using Eqs. (4), (6) and (7).

On Table 2, we present the different calculated values of R, N_{phe}, R_M and R_i for different sample detectors. The sample detector annealed under vacuum atmosphere exhibits the better energy resolution compared to the samples annealed at air and nitrogen. The number of photoelectrons N_{phe} is higher for the YAG_Vacuum detector which can be connected with increasing the crystallite size by changing the treatment atmosphere, R_M remains practically constant, R_i decreases with crystallite size, one can think that the improvement of R is related to R_i.

The most important factor that can alter the energy resolution is the non-proportionality of the light yield. It acts by many secondary gamma and X-ray quanta and scattering of secondary electrons. A study suggests a correlation between the impurities in the crystal and the intrinsic resolution, a pure crystal can give a better energy resolution [56].

In fact, the calcination under vacuum allow to get YAG: Ce nanopowder with a large size of crystallite compared to that obtained under air and nitrogen atmospheres [33], this can improve the crystal quality and decrease the contributions of the non-proportionality and non-homogeneity responses.

Scintillation decay time

Room temperature scintillation decay curves of studied samples were measured under γ-rays from ^{137} Cs radioactive source and presented in Fig. 8, the decay curves were well fitted by the following equation:

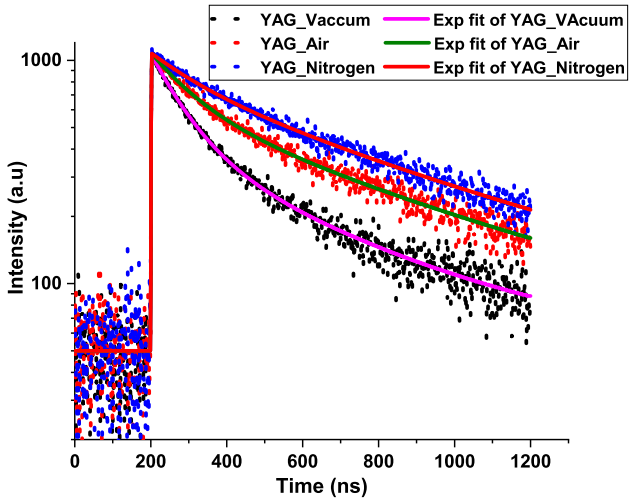

Fig. 8 Scintillation decay time of studied sample detectors under ^{137}Cs γ-rays

$$I(t) = A_f e^{-t/\tau_f} - A_r e^{-t/\tau_r} + A_s e^{-t/\tau_s} + y_0 \quad (8)$$

where τ_f and τ_s are, respectively, the decay time constants of the fast and slow components, τ_r is the rise time constant. A_f, A_s and A_r are the corresponding intensities. The decay time components with their corresponding fractional intensity ratios and the rise time are summarized in Table 3.

From the obtained results, one can observe that the sample YAG_Vacuum shows the fast decay time with higher relative intensity compared to the samples YAG_Air and YAG_Nitrogen. Also, it was noted that the scintillation decay time of the sample YAG_Vacuum was slightly better than that of YAG: Ce single crystal reported in refs [6, 19].

The improvement of the scintillation decay time may be related to the decrease of the defect density. Additionally, the higher intensity of fast component can be due to the decrease of re-trapping of free charge carriers at shallow trap when vacuum is used as annealing atmosphere.

Conclusion

In this paper, the effect of the calcination atmosphere on the scintillation properties of YAG: Ce^{3+} nanopowder has been investigated under γ-ray 662 keV excitation. The results showed that the annealing atmospheres can strongly affect the scintillation properties. The sample YAG_Vacuum with 1 mm thickness exhibits the best characteristics compared to YAG_Air and YAG_Nitrogen samples. Consequently, the vacuum annealing is a suitable method for developing YAG: Ce^{3+} nanoscintillators for use in radiation detection applications. Future work will focus on investigating the impact of additional parameters, such as annealing temperature and pH of the solution used during the elaboration of YAG: Ce^{3+} nanophosphor. Furthermore, besides their use as standalone detectors, the evaluation of sample detectors in powder form is a crucial step in identifying the optimal synthesis conditions. By conducting this initial assessment, we can streamline the development of transparent scintillator ceramics that hold significant potential for future applications, thereby paving the way for further research in this field. Moreover, mixed doping is another promising approach for achieving high optical output in scintillator materials. For instance, it has been reported that mixed doping can result in an optical output of 4×10^4 ph/MeV, making it a significant research direction for crystal powder applications.

Declarations

Conflict of interest Conflict of interest on behalf of all authors, the corresponding author states that there is no conflict of interest.

References

1. A. Tarafder, A.R. Molla, B. Karmakar, Chapter 13—advanced glass-ceramic nanocomposites for structural, photonic, and optoelectronic applications, in *Glass Nanocomposites*. ed. by B. Karmakar, K. Rademann, A.L.B.T.-G.N. Stepanov (William Andrew Publishing, Boston, 2016), pp.299–338
2. Y.-C. Wu, S. Parola, O. Marty et al., Structural characterizations and waveguiding properties of YAG thin films obtained by different sol–gel processes. Opt. Mater. (Amst.) **27**, 1471–1479 (2005). https://doi.org/10.1016/j.optmat.2005.03.004
3. H.M.H. Fadlalla, C.C. Tang, S.Y. Wei, X.X. Ding, Preparation and properties of nanocrystalline powders in $(Y_{1-x}Ce_x)_3Al_5O_{12}$ system. J. Lumin. **128**, 1655–1659 (2008). https://doi.org/10.1016/j.jlumin.2008.03.018
4. H.M.H. Fadlalla, C. Tang, Sol–gel preparation and photoluminescence properties of Ce^{3+}-activated $Y_3Al_5O_{12}$ nano-sized powders. J. Cryst. Growth **311**, 3737–3741 (2009). https://doi.org/10.1016/j.jcrysgro.2009.04.040
5. T. Ji, T. Wang, H. Li et al., Ce^{3+}-doped yttrium aluminum garnet transparent ceramics for high-resolution X-ray imaging. Adv. Opt. Mater. (2022). https://doi.org/10.1002/adom.202102056
6. M. Kim, H.J. Kim, J.Y. Cho et al., Crystal growth and scintillation properties of YAG: Ce^{3+} for γ and α detection. Appl. Radiat. Isot. **145**, 126–130 (2019). https://doi.org/10.1016/j.apradiso.2018.12.011
7. Y. Yan, C. Zhang, L. Zheng et al., Dosimeter based on YAG: Ce phosphor via sol-gel method for online X-ray radiation monitoring. Curr. Comput. Aided Drug Des. **11**, 1567 (2021). https://doi.org/10.3390/cryst11121567
8. D. Valiev, V. Vaganov, T. Han, et al., Time-resolved luminescence of YAG: Ce^{3+}, Tb^{3+} ceramics. in *AIP Conference Proceedings*. (AIP Publishing LLC, 2019), pp. 20263
9. A. Speghini, F. Piccinelli, M. Bettinelli, Synthesis, characterization and luminescence spectroscopy of oxide nanopowders activated with trivalent lanthanide ions: the garnet family. Opt.

Mater. (Amst) **33**, 247–257 (2011). https://doi.org/10.1016/j.optmat.2010.10.039
10. W.T. Hong, J.H. Lee, J.W. Son et al., Color rendering improvement of the YAG: Ce^{3+} phosphors by co-doping with Gd^{3+} ions. Ceram. Int. **42**, 2204–2208 (2016). https://doi.org/10.1016/j.ceramint.2015.10.010
11. J. Jia, Y. Qiang, J. Xu et al., A comparison study on the substitution of $Y^{3+}-Al^{3+}$ by $M^{2+}-Si^{4+}$ (M=Ba, Sr, Ca, Mg) in $Y_3Al_5O_{12}$: Ce^{3+} phosphor. J. Am. Ceram. Soc. **103**, 5111–5119 (2020). https://doi.org/10.1111/jace.17204
12. M.A. Almessiere, N.M. Ahmed, I. Massoudi et al., Study of the structural and luminescent properties of Ce^{3+} and Eu^{3+} co-doped YAG synthesized by solid state reaction. Optik (Stuttg) **158**, 152–163 (2018). https://doi.org/10.1016/j.ijleo.2017.12.031
13. M.V. Derdzyan, K.L. Hovhannesyan, A.V. Yeganyan et al., Dissimilar behavior of YAG: Ce and LuAG: Ce scintillator garnets regarding Li^+ co-doping. Cryst. Eng. Comm. **20**, 1520–1526 (2018). https://doi.org/10.1039/C7CE02194A
14. M. Jia, J. Wen, W. Luo et al., Improved scintillating properties in Ce: YAG derived silica fiber with the reduction from Ce^{4+} to Ce^{3+} ions. J. Lumin. **221**, 117063 (2020). https://doi.org/10.1016/j.jlumin.2020.117063
15. Q. Wang, B. Yang, Y. Zhang et al., High light yield Ce^{3+}-doped dense scintillating glasses. J. Alloys Compd. **581**, 801–804 (2013). https://doi.org/10.1016/j.jallcom.2013.07.181
16. O. Sidletskiy, K. Lebbou, D. Kofanov et al., Progress in fabrication of long transparent YAG: Ce and YAG: Ce, Mg single crystalline fibers for HEP applications. Cryst. Eng. Comm. **21**, 1728–1733 (2019). https://doi.org/10.1039/C8CE01781F
17. Z. Jiuping, L. Hongbin, S. Qiang et al., Effects of annealing treatments on luminescence and scintillation properties of Ce: $Lu_3Al_5O_{12}$ crystal grown by Czochralski method. J. Rare Earths **25**, 568–572 (2007). https://doi.org/10.1016/S1002-0721(07)60564-X
18. S. Chen, B. Jiang, Q. Zhu et al., A effect of annealing atmosphere on scintillation properties of GYGAG: Ce, Mg scintillator ceramics. Nuclear Inst. Methods Phys. Res. **942**, 0–4 (2019). https://doi.org/10.1016/j.nima.2019.162360
19. W. Chewpraditkul, L. Swiderski, M. Moszynski et al., Comparative studies of $Lu_3Al_5O_{12}$: Ce and $Y_3Al_5O_{12}$: Ce scintillators for gamma-ray detection. Phys. Status Solidi Appl. Mater. Sci. **206**, 2599–2605 (2009). https://doi.org/10.1002/pssa.200925161
20. C. Zhang, J. Lin, Defect-related luminescent materials: synthesis, emission properties and applications. Chem. Soc. Rev. **41**, 7938–7961 (2012). https://doi.org/10.1039/C2CS35215J
21. C.B. Carter, M.G. Norton, *Ceramic materials: science and engineering* (Springer, London, 2007)
22. G. Blasse, Scintillator materials. Chem. Mater. **6**, 1465–1475 (1994)
23. C. Greskovich, S. Duclos, Ceramic scintillators. Annu. Rev. Mater. Sci. **27**, 69–88 (1997)
24. L. Yang, T. Lu, H. Xu, N. Wei, Synthesis of YAG powder by the modified sol–gel combustion method. J. Alloys. Compd. **484**, 449–451 (2009). https://doi.org/10.1016/j.jallcom.2009.04.123
25. F. Yuan, H. Ryu, Ce-doped YAG phosphor powders prepared by co-precipitation and heterogeneous precipitation. Mater. Sci. Eng. B **107**, 14–18 (2004). https://doi.org/10.1016/j.mseb.2003.10.002
26. N. Jia, X. Zhang, W. He et al., Property of YAG: Ce phosphors powder prepared by mixed solvothermal method. J. Alloys Compd. **509**, 1848–1853 (2011). https://doi.org/10.1016/j.jallcom.2010.10.071
27. S.-K. Ruan, J.-G. Zhou, A.-M. Zhong et al., Synthesis of $Y_3Al_5O_{12}$: Eu^{3+} phosphor by sol-gel method and its luminescence behavior. J. Alloys Compd. **275**, 72–75 (1998). https://doi.org/10.1016/S0925-8388(98)00276-X
28. A. Boukerika, L. Guerbous, N. Brihi, Ce-doped YAG phosphors prepared via sol–gel method: effect of some modular parameters. J. Alloys Compd. **614**, 383–388 (2014). https://doi.org/10.1016/j.jallcom.2014.06.133
29. S.K. Gupta, Y. Mao, Recent advances, challenges, and opportunities of inorganic nanoscintillators. Front. Optoelectron. **13**, 156–187 (2020). https://doi.org/10.1007/s12200-020-1003-5
30. A. Magi, M. Koshimizu, A. Watanabe et al., Optimization of phosphor concentration of surface-modified Bi_2O_3 nanoparticle loaded plastic scintillators for high energy photon detection. J. Mater. Sci. Mater. Electron **32**, 7987–7999 (2021). https://doi.org/10.1007/s10854-021-05522-4
31. J. Janda, The comparison of scintillation properties of YAP: Ce, YAG: Ce and ZnO: Ga powders as a potential substitution of LSC cocktail. J. Radioanal. Nucl. Chem. **314**, 573–582 (2017). https://doi.org/10.1007/s10967-017-5376-x
32. L. Guerbous, A. Boukerika, Nanomaterial host bands effect on the photoluminescence properties of Ce-doped YAG nanophosphor synthesized by sol-gel method. J. Nanomater. **2**, 1–10 (2015). https://doi.org/10.1155/2015/617130
33. A. Boukerika, L. Guerbous, M. Belamri, Effect of different annealing atmospheres on the structural and luminescence properties of Ce^{3+}-doped YAG phosphors synthesized by sol–gel method. Optik (Stuttg) **127**, 5235–5239 (2016). https://doi.org/10.1016/j.ijleo.2016.03.037
34. G.K. de Oliveira, F.R. de Oliveira Silva, D.P. Vieira, L.C. Courrol, Synthesis and characterization of aminolevulinic acid with gold and iron nanoparticles by photoreduction method for non-communicable diseases diagnosis and therapy. J. Mater. Sci. Mater. Electron **30**, 16789–16797 (2019). https://doi.org/10.1007/s10854-019-01337-6
35. P. Agostinis, K. Berg, K.A. Cengel et al., Photodynamic therapy of cancer: an update. CA Cancer J. Clin. **61**, 250–281 (2011). https://doi.org/10.20517/2394-4722.2018.83
36. J.M. Dąbrowski, L.G. Arnaut, Photodynamic therapy (PDT) of cancer: from local to systemic treatment. Photochem. Photobiol. Sci. **14**, 1765–1780 (2015). https://doi.org/10.1039/c5pp00132c
37. W. Chen, J. Zhang, Using nanoparticles to enable simultaneous radiation and photodynamic therapies for cancer treatment. J. Nanosci. Nanotechnol. **6**, 1159–1166 (2006). https://doi.org/10.1166/jnn.2006.327
38. N.Y. Morgan, G. Kramer-Marek, P.D. Smith et al., Nanoscintillator conjugates as photodynamic therapy-based radiosensitizers: calculation of required physical parameters. Radiat. Res. **171**, 236–244 (2009). https://doi.org/10.1667/RR1470.1
39. W. Sun, Z. Zhou, G. Pratx, H.C. Xiaoyuan Chen, Nanoscintillator-mediated X-ray induced photodynamic therapy for deep-seated tumors: from concept to biomedical applications. Theranostics **10**, 1296–1318 (2020). https://doi.org/10.7150/thno.41578
40. P. Sengar, P. Juárez, A. Verdugo-Meza et al., Development of a functionalized UV-emitting nanocomposite for the treatment of cancer using indirect photodynamic therapy. J. Nanobiotechnol. **16**, 1–19 (2018). https://doi.org/10.1186/s12951-018-0344-3
41. A. Jain, R. Koyani, C. Muñoz et al., Magnetic-luminescent cerium-doped gadolinium aluminum garnet nanoparticles for simultaneous imaging and photodynamic therapy of cancer cells. J. Colloid Interface Sci. **526**, 220–229 (2018). https://doi.org/10.1016/j.jcis.2018.04.100
42. L.M. Bollinger, G.E. Thomas, Measurement of the time dependence of scintillation intensity by a delayed-coincidence method. Rev. Sci. Instrum. **32**, 1044–1050 (1961). https://doi.org/10.1063/1.1717610
43. J. Qin, C. Lai, J. Xiao et al., Characteristics and time resolutions of two $CeBr_3$ gamma-ray spectrometers. Radiat. Detect.

Technol. Methods **4**, 327–336 (2020). https://doi.org/10.1007/s41605-020-00187-9
44. M. Moszynski, M. Kapusta, M. Mayhugh et al., Absolute light output of scintillators. IEEE Trans. Nucl. Sci. **44**, 1052–1061 (1997). https://doi.org/10.1109/23.603803
45. E. Sysoeva, V. Tarasov, O. Zelenskaya, Comparison of the methods for determination of scintillation light yield. Nucl. Instrum. Methods Phys. Res. Sect. A Accel. Spectrom. Detect. Assoc. Equip. **486**, 67–73 (2002). https://doi.org/10.1016/S0168-9002(02)00676-9
46. M. Gierlik, M. Moszynski, A. Nassalski et al., Investigation of absolute light. IEEE Trans. Nucl. Sci. **54**, 1367–1371 (2007)
47. M. Moszyński, M. Kapusta, M. Mayhugh et al., Absolute light output of scintillators. IEEE Trans. Nucl. Sci. **44**, 1052–1061 (1997). https://doi.org/10.1109/23.603803
48. V. Jarý, J. Pejchal, Scintillators around us, Center of Administration and Operation CAS, v. v. i. Layout: Jakub Krč; Type: Serifa. in 1st edn., ed. by P. Královcová. (Institute of physics of the Czech Academy of Sciences, 2018), pp. 12413
49. C.W.E. Eijk, Inorganic scintillators in medical imaging. Phys. Med. Biol. **47**, R85-106 (2002). https://doi.org/10.1088/0031-9155/47/8/201
50. M. Nikl, Scintillation detectors for X-rays. Meas. Sci. Technol. **17**, R37 (2006). https://doi.org/10.1088/0957-0233/17/4/R01
51. C. Dujardin, D. Amans, A. Belsky et al., Luminescence and scintillation properties at the nanoscale. IEEE Trans. Nucl. Sci. **57**, 1348–1354 (2010). https://doi.org/10.1109/TNS.2009.2035697
52. P. Dorenbos, J.T.M. de Haas, C.W.E. Van Eijk, Non-proportionality in the scintillation response and the energy resolution obtainable with scintillation crystals. IEEE Trans. Nucl. Sci. **42**, 2190–2202 (1995). https://doi.org/10.1016/j.nima.2015.07.059
53. Shah KS (2010) New scintillation detectors for PET. Dr Delft Univ Technol 259:
54. P. Dorenbos, Light output and energy resolution of Ce^{3+}-doped scintillators. Nucl. Instrum. Methods Phys. Res. Sect. A Accel. Spectrom. Detect. Assoc. Equip. **486**, 208–213 (2002). https://doi.org/10.1016/S0168-9002(02)00704-0
55. E.B. Johnson, C.J. Stapels, X.J. Chen, et al. CMOS solid-state photomultipliers for high energy resolution calorimeters. in *Hard X-Ray, Gamma-Ray, and Neutron Detector Physics XIII*. (SPIE, 2011), pp. 127–140
56. M. Moszyński, Energy resolution and non-proportionality of scintillation detectors–new observations. Radiat. Meas. **45**, 372–376 (2010)